

Empirical Structural Design of Au@Ag Nanoparticles for SERS Applications

Yijing Li,^a Qiurong Shi,^a Peina Zhang,^a Yujiao Xiahou,^a Shuzhou Li,^c Dayang Wang^b and
Haibing Xia,^{*a}

^a*State Key Laboratory of Crystal Materials, Shandong University, Jinan, 250100, P. R China.*

^b*Department of Civil, Environmental, and Chemical Engineering, School of Engineering, RMIT
University, VIC 3001, Australia.*

^c*School of Materials Science and Engineering, Nanyang Technological University, Singapore
639798*

E-mail: hbxia@sdu.edu.cn

Fig. S1 TEM images (a to i in A), extinction spectra (a to i in B), and digital photographs (a to i in C) of citrate stabilized 12 nm Au NPs (a), Au₁₂@Ag_{1.1} NPs (b), Au₁₂@Ag_{1.8} NPs (c), Au₁₂@Ag_{2.1} NPs (d), Au₁₂@Ag_{2.5} NPs (e), Au₁₂@Ag_{2.9} NPs (f), Au₁₂@Ag_{3.3} NPs (g), Au₁₂@Ag_{4.0} NPs (h), and Au₁₂@Ag_{4.6} NPs (i). The experimental details are listed in Table S2.

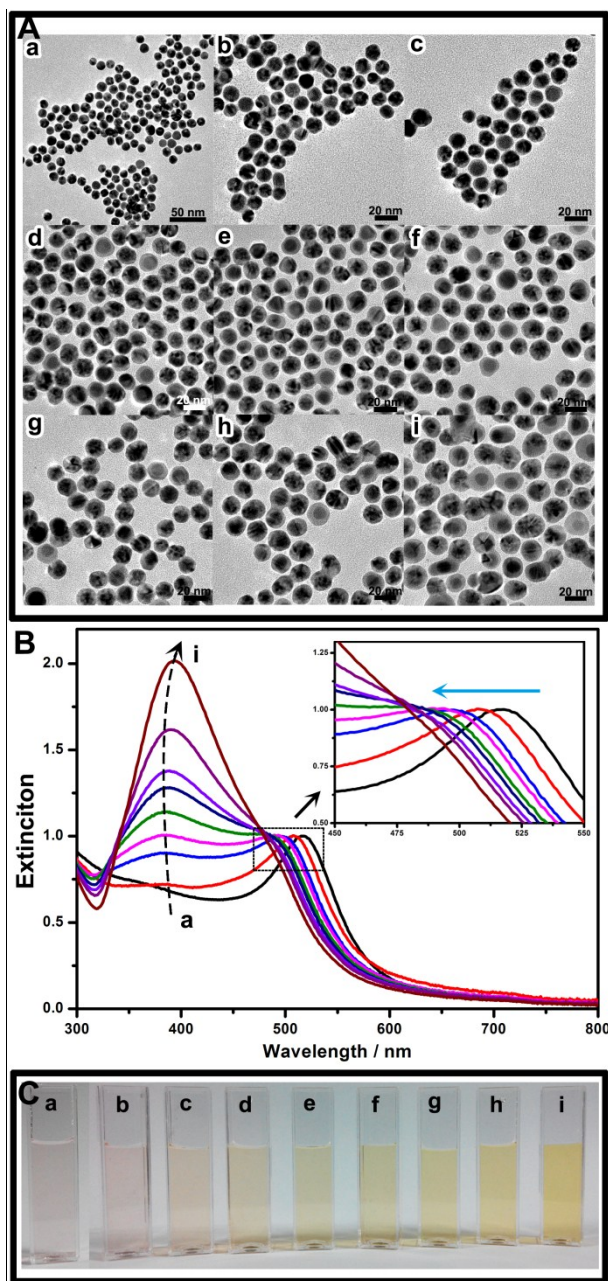


Fig. S2 TEM images (a to i in A), extinction spectra (a to i in B), and digital photographs (a to i in C) of citrate stabilized 30 nm Au NPs (a), Au₃₀@Ag_{1.7} NPs (b), Au₃₀@Ag_{3.6} NPs (c), Au₃₀@Ag_{5.0} NPs (d), Au₃₀@Ag_{6.0} NPs (e), Au₃₀@Ag_{6.4} NPs (f), Au₃₀@Ag_{7.0} NPs (g), Au₃₀@Ag_{9.8} NPs (h), and Au₃₀@Ag_{12.0} NPs (i). The experimental details are listed in Table S3.

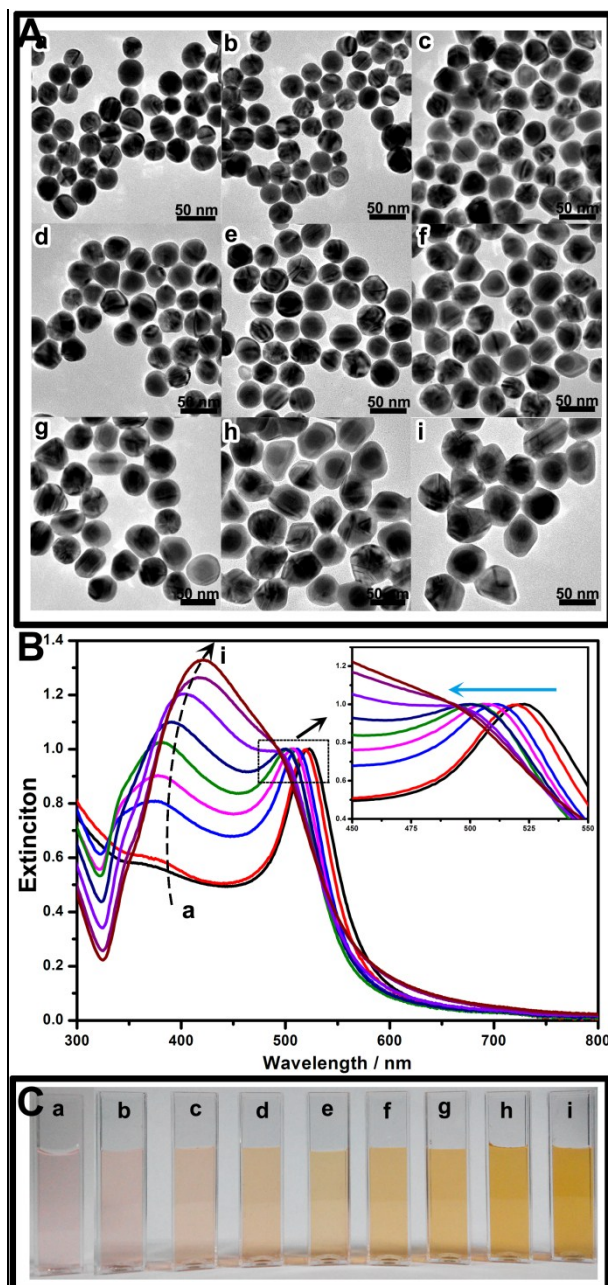


Fig. S3 TEM images (a to g in A), extinction spectra (a to g in B), and digital photographs (a to g in C) of citrate stabilized 45 nm Au NPs (a), Au₄₅@Ag_{0.9} NPs (b), Au₄₅@Ag_{1.5} NPs (c), Au₄₅@Ag_{2.9} NPs (d), Au₄₅@Ag_{5.5} NPs (e), Au₄₅@Ag_{8.2} NPs (f), and Au₄₅@Ag_{11.0} NPs (g). The experimental details are listed in Table S4.

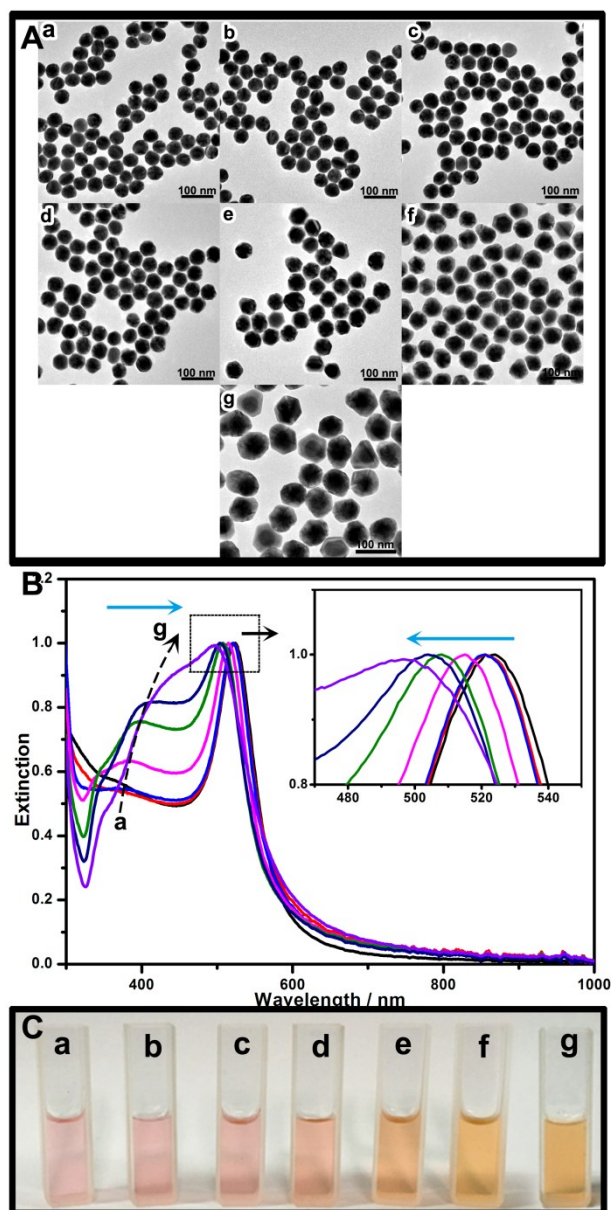


Fig. S4 TEM images (a to f in A), extinction spectra (a to f in B), and digital photographs (a to f in C) of citrate stabilized 55 nm Au NPs (a), Au₅₅@Ag_{0.8} NPs (b), Au₅₅@Ag_{2.7} NPs (c), Au₅₅@Ag_{5.0} NPs (d), Au₅₅@Ag_{10.0} NPs (e), and Au₅₅@Ag_{16.0} NPs (f). The experimental details are listed in Table S5.

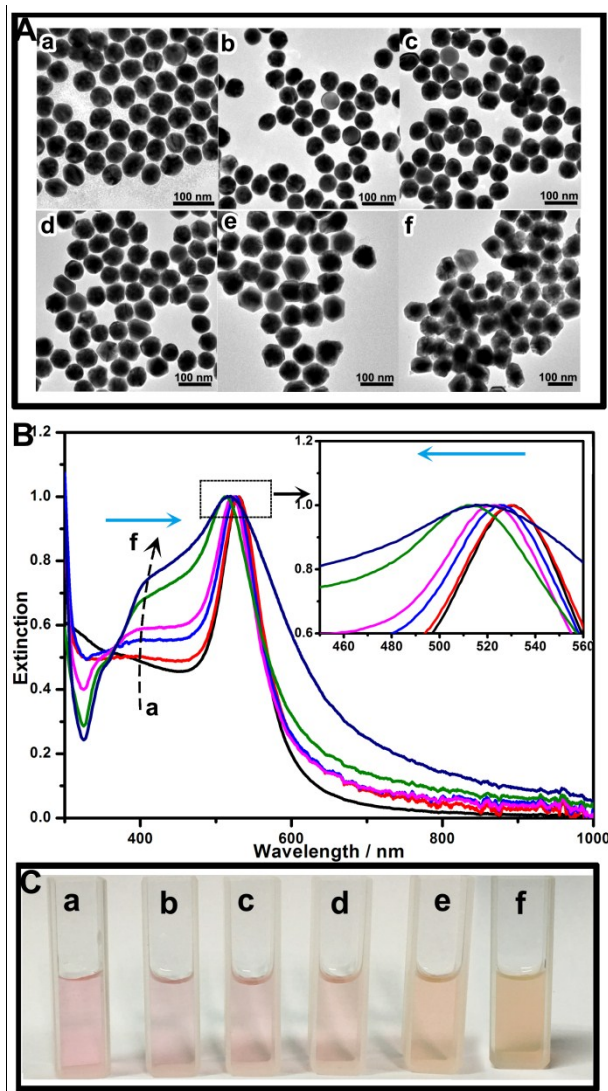


Fig. S5 Experimental extinction spectrum (a) and TEM image (b) of 29 nm Ag NPs synthesized by AA/citrate reduction protocol.

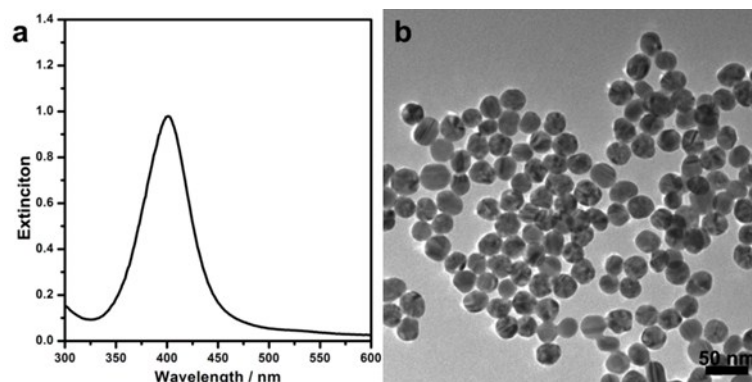


Fig. S6 TEM images of citrate stabilized 20 nm Au NPs (a), Au₂₀@Ag_{1.6} NPs (b), Au₂₀@Ag_{2.1} NPs (c), Au₂₀@Ag_{2.8} NPs (d), Au₂₀@Ag_{3.7} NPs (e), Au₂₀@Ag_{4.5} NPs (f), Au₂₀@Ag_{5.5} NPs (g), Au₂₀@Ag_{7.0} NPs (h), and Au₂₀@Ag_{9.0} NPs (i).

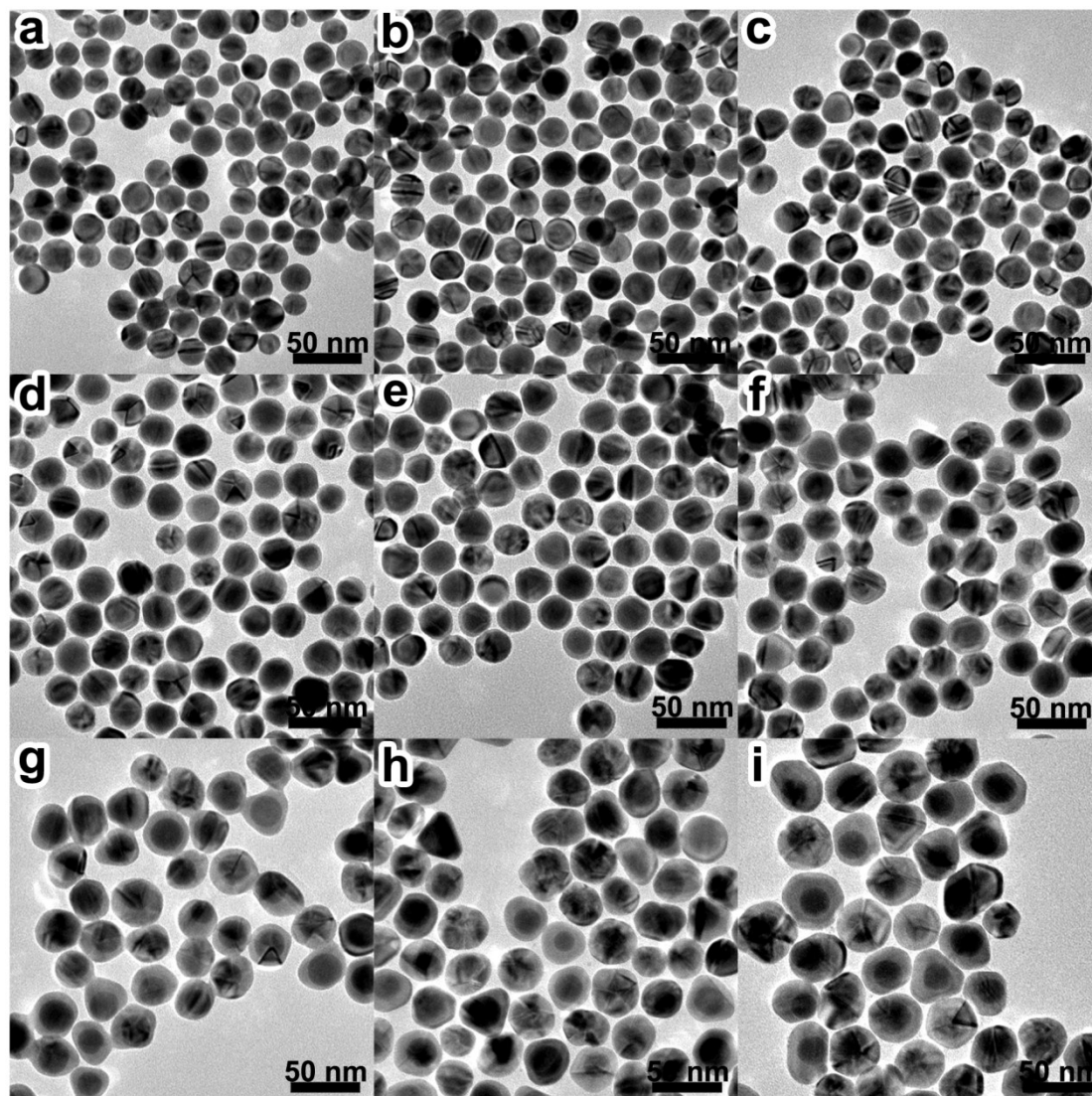


Fig. S7 HAADF-STEM image (a), energy dispersive X-ray spectrometer (EDS) spectrum (b) of CS Au₂₀@Ag_{4.5} NPs and cross-sectional compositional line profile of one single CS Au₂₀@Ag_{4.5} NP (c).

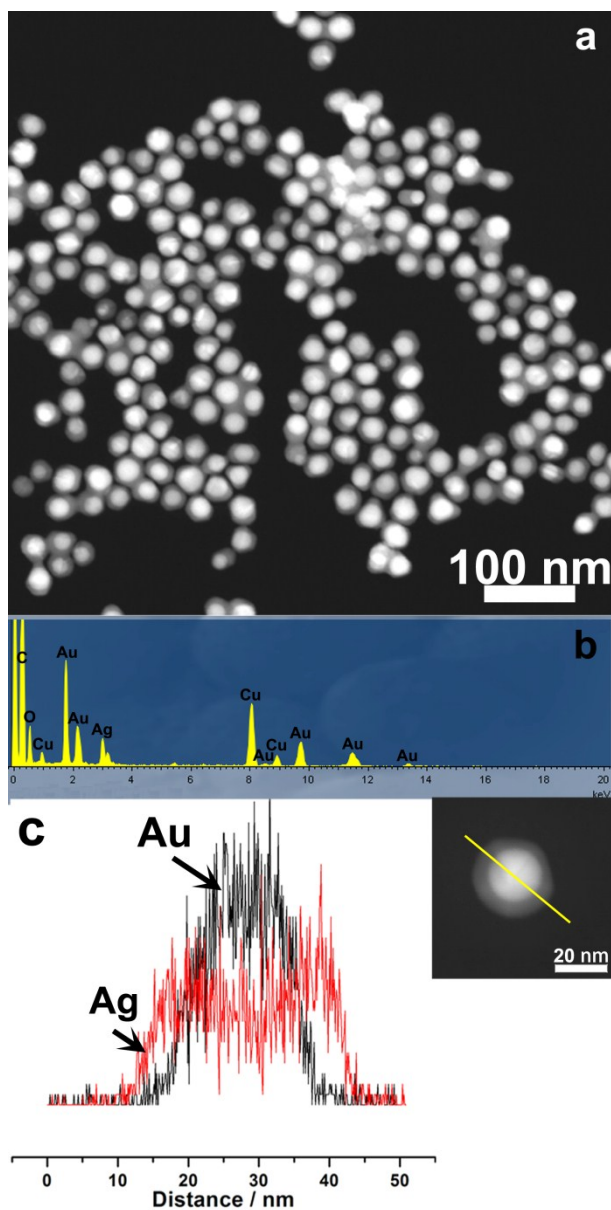


Fig. S8 Normal Raman spectrum of the neat film of 4-ATP molecule and SERS spectrum of 4-ATP molecules absorbed on film of 29 nm Ag NP. The excitation laser wavelength for Raman measurements is 633 nm. The acquisition time was 2 s.

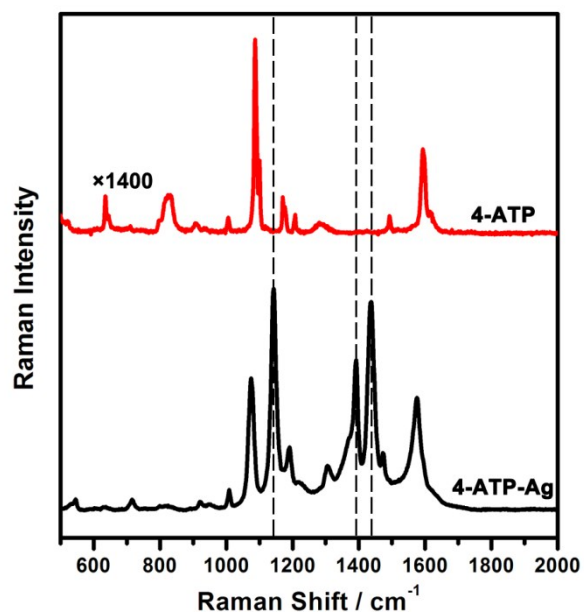


Fig. S9 SERS spectra of 4-ATP molecules (3×10^{-4} M) absorbed on the film of Au₁₂@Ag_{1.1} NPs (a), Au₁₂@Ag_{1.8} NPs (b), Au₁₂@Ag_{2.1} NPs (c), Au₁₂@Ag_{2.5} NPs (d), Au₁₂@Ag_{2.9} NPs (e), Au₁₂@Ag_{4.0} NPs (f), and Au₁₂@Ag_{4.6} NPs (g), cast on glass substrates. The excitation laser wavelength for Raman measurements is 633 nm and the acquisition time is 2 s.

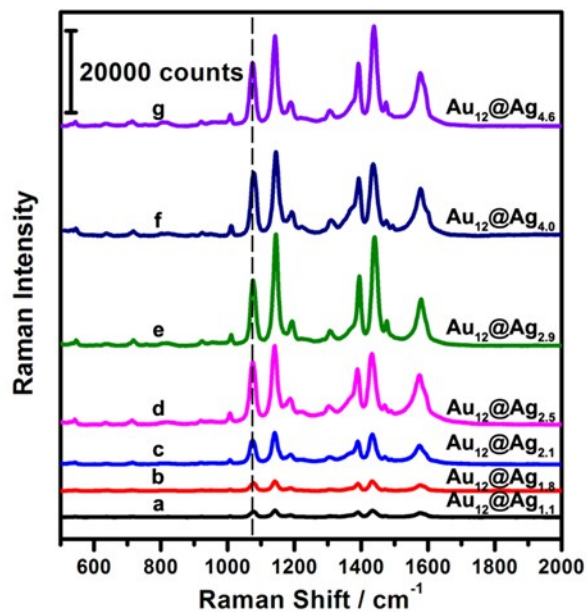


Fig. S10 SERS spectra of 4-ATP molecules (3×10^{-4} M) absorbed on the film of Au₃₀@Ag_{1.7} NPs (a), Au₃₀@Ag_{3.6} NPs (b), Au₃₀@Ag_{5.0} NPs (c), Au₃₀@Ag_{6.4} NPs (d), Au₃₀@Ag_{9.8} NPs (e), and Au₃₀@Ag_{12.0} NPs (f), cast on glass substrates. The excitation laser wavelength for Raman measurements is 633 nm and the acquisition time is 2 s.

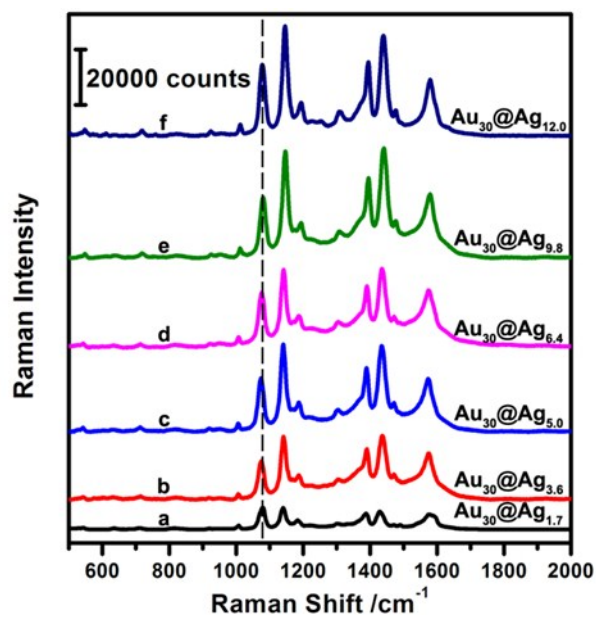


Fig. S11 SERS spectra of 4-ATP molecules (3×10^{-4} M) absorbed on the film of 45 nm Au NPs (a), Au₄₅@Ag_{0.9} NPs (b), Au₄₅@Ag_{1.5} NPs (c), Au₄₅@Ag_{2.9} NPs (d), Au₄₅@Ag_{5.5} NPs (e), Au₄₅@Ag_{8.2} NPs (f), and Au₄₅@Ag_{11.0} NPs (g), cast on glass substrates. The excitation laser wavelength for Raman measurements is 633 nm and the acquisition time is 5 s.

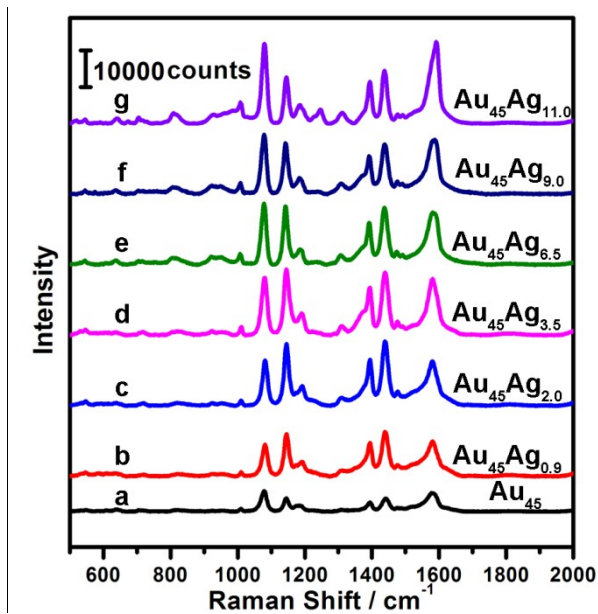


Fig. S12 SERS spectra of 4-ATP molecules (3×10^{-4} M) absorbed on the film of 55 nm Au NPs (a), Au₅₅@Ag_{0.8} NPs (b), Au₅₅@Ag_{2.7} NPs (c), Au₅₅@Ag_{5.0} NPs (d), Au₅₅@Ag_{10.0} NPs (e), and Au₅₅@Ag_{16.0} NPs (f), cast on glass substrates. The excitation laser wavelength for Raman measurements is 633 nm and the acquisition time is 2 s.

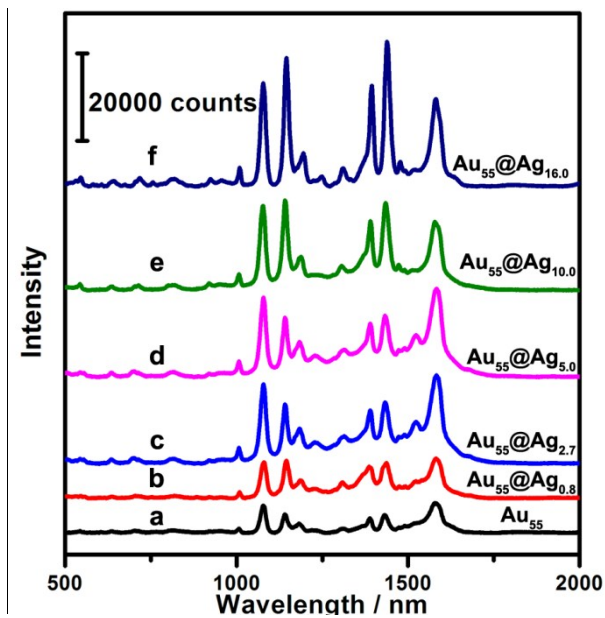


Fig. S13. Experimental extinction spectra of CS Au_{2r}@Ag_t NPs of different sizes on glass substrates (samples in Fig. 7).

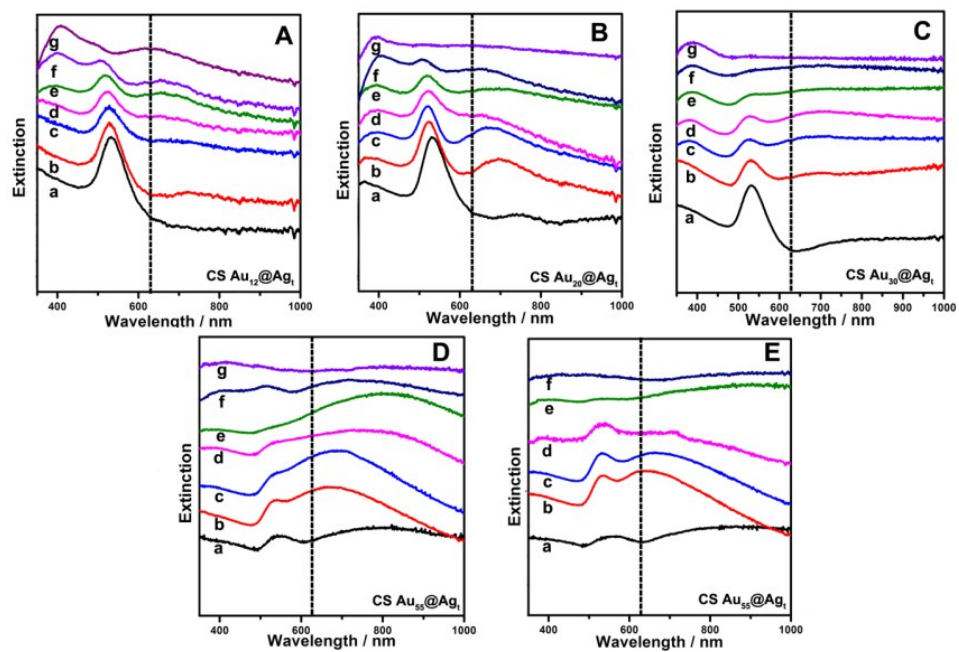


Fig. S14 Imaginary components of “bulk” dielectric constants of gold and silver clusters.

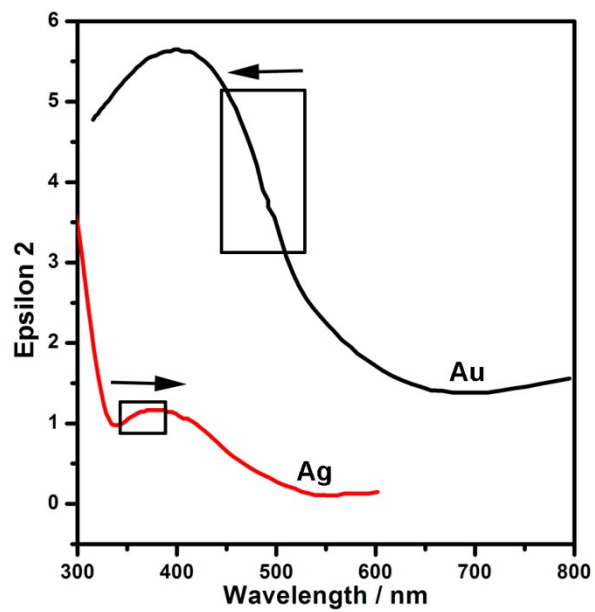


Table S1 Summary of the experimental parameters used for synthesis of citrate stabilized Au NPs of 12, 20, 30, 45, and 55 nm *via* tuning the amounts of citrate (1 wt %), and HAuCl₄ (1 wt %) at the fixed AgNO₃ concentration (0.1 wt %) and tuning the incubation time.

Diameters of Au NPs (nm)	H ₂ O (mL)	Citrate (mL)	HAuCl ₄ (mL)	AgNO ₃ (μL)	Incubation time (min)
12	0.50	1.50	0.50	42.5	5.0
20	0.85	0.90	0.75	42.5	5.5
30	1.10	0.65	0.75	42.5	4.5
45	0.50	0.50	0.50	42.5	4.5
55	0.60	0.40	0.50	42.5	4.0

Table S2 Summary of the experimental details used for synthesis of CS Au₁₂@Ag_t NPs *via* Ag overgrowth on as-prepared Au NPs with diameters of 12 ± 1 nm as seeds.

Sample image	H ₂ O (mL)	Citrate (mL)	Au NPs (mL)	AA (μL)	AgNO ₃ (μL)	t (nm)	Adsorption position of Au cores (nm)	Adsorption position of Ag shells (nm)
Figure S1a	8.700	0.3	1	-	-	-	517	-
Figure S1b	8.680	0.3	1	10	10	1.1	508	-
Figure S1c	8.670	0.3	1	10	20	1.8	497	381
Figure S1d	8.655	0.3	1	20	25	2.1	493	383
Figure S1e	8.650	0.3	1	20	30	2.5	489	384
Figure S1f	8.645	0.3	1	20	35	2.9	485	387
Figure S1g	8.640	0.3	1	20	40	3.3	480	389
Figure S1h	8.625	0.3	1	25	50	4.0	-	390
Figure S1i	8.595	0.3	1	35	70	4.6	-	393

Table S3 Summary of the experimental details used for synthesis of CS Au₃₀@Ag_t NPs *via* Ag overgrowth on as-prepared Au NPs with diameters of 30 ± 3 nm as seeds.

Sample image	H ₂ O (mL)	Citrate (mL)	Au NPs (mL)	AA (μL)	AgNO ₃ (μL)	t (nm)	Adsorption position of Au cores (nm)	Adsorption position of Ag shells (nm)
Figure S2a	8.700	0.3	1	-	-	-	522	-
Figure S2b	8.680	0.3	1	10	10	1.7	519	380
Figure S2c	8.655	0.3	1	10	20	3.6	511	375
Figure S2d	8.655	0.3	1	15	30	5.0	507	377
Figure S2e	8.640	0.3	1	20	40	6.0	502	381
Figure S2f	8.625	0.3	1	25	50	6.4	498	388
Figure S2g	8.595	0.3	1	35	70	7.0	490	402
Figure S2h	8.535	0.3	1	55	110	9.8	-	411
Figure S2i	8.475	0.3	1	75	150	12.0	-	422

Table S4 Summary of the experimental details used for synthesis of CS Au₄₅@Ag_t NPs *via* Ag overgrowth on as-prepared Au NPs with diameters of 45 ± 3 nm as seeds.

Sample image	H ₂ O (mL)	Citrate (mL)	Au NPs (mL)	HQ (μL)	AgNO ₃ (μL)	t (nm)	Adsorption position of Au cores (nm)	Adsorption position of Ag shells (nm)
Figure S3a	8.700	0.3	1	-	-	-	524	-
Figure S3b	8.685	0.3	1	10	5	0.9	522	366
Figure S3c	8.680	0.3	1	10	10	1.5	521	377
Figure S3d	8.660	0.3	1	20	20	2.9	515	383
Figure S3e	8.640	0.3	1	20	40	5.5	508	396
Figure S3f	8.610	0.3	1	30	60	8.2	505	404
Figure S3g	8.520	0.3	1	60	120	11.0	496	440

Table S5 Summary of the experimental details used for synthesis of CS Au₅₅@Ag_t NPs *via* Ag overgrowth on as-prepared Au NPs with diameters of 55 ± 3 nm as seeds.

Sample image	H ₂ O (mL)	Citrate (mL)	Au NPs (mL)	HQ (μL)	AgNO ₃ (μL)	t (nm)	Adsorption position of Au cores (nm)	Adsorption position of Ag shells (nm)
Figure S4a	8.700	0.3	1	-	-	-	531	-
Figure S4b	8.685	0.3	1	10	5	0.8	530	375
Figure S4c	8.680	0.3	1	10	10	2.7	526	389
Figure S4d	8.660	0.3	1	20	20	5.0	522	395
Figure S4e	8.610	0.3	1	30	60	10.0	513	398
Figure S4f	8.520	0.3	1	60	120	16.0	516	413

Table S6 Crystal lattice distance of fcc Au and Ag.

	(111)	(200)	(220)
Au	0.235 nm	0.204 nm	0.144 nm
Ag	0.236 nm	0.204 nm	0.144 nm

Table S7 Intensities of main SERS bands between 500 and 2000 cm^{-1} of 4-ATP molecules absorbed on film of 30 nm Au NPs on glass substrates. The excitation laser wavelengths for SERS measurements are 473, 633, and 785 nm, respectively. The acquisition time is 2 s.

Excitation laser wavelength (nm)	Intensities of main SERS bands of 4-ATP molecules and their position (cm^{-1})				
473	-	-	-	-	-
633	4925 at 1078 cm^{-1}	6085 at 1142 cm^{-1}	4396 at 1390 cm^{-1}	5784 at 1433 cm^{-1}	3800 at 1576 cm^{-1}
785	278 at 1082 cm^{-1}	48 at 1146 cm^{-1}	43 at 1388 cm^{-1}	41 at 1434 cm^{-1}	130 at 1591 cm^{-1}

Table S8 Intensities of main SERS bands between 500 and 2000 cm^{-1} of 4-ATP molecules absorbed on film of 29 nm Ag NPs on glass substrates. The excitation laser wavelengths for SERS measurements are 473, 633, and 785 nm, respectively. The acquisition time is 2 s.

Excitation laser wavelength (nm)	Intensities of main SERS bands of 4-ATP molecules and their position (cm^{-1})				
473	3519 at	6245 at	9171 at	14687 at	6681 at
	1089 cm^{-1}	1154 cm^{-1}	1403 cm^{-1}	1449 cm^{-1}	1589 cm^{-1}
633	19148 at	32161 at	21752 at	30221 at	16319 at
	1075 cm^{-1}	1142 cm^{-1}	1391 cm^{-1}	1437 cm^{-1}	1575 cm^{-1}
785	1220 at	567 at	407 at	408 at	414 at
	1081 cm^{-1}	1142 cm^{-1}	1390 cm^{-1}	1434 cm^{-1}	1595 cm^{-1}

Table S9 Intensities of main SERS bands between 500 and 2000 cm^{-1} of 4-ATP molecules absorbed on film of CS Au₂₀@Ag_{4.5} NPs on glass substrates. The excitation laser wavelengths for SERS measurements are 473, 633, and 785 nm, respectively. The acquisition time is 2 s.

Excitation laser wavelength (nm)	Intensities of main SERS bands of 4-ATP molecules and their position (cm^{-1})				
473	1012 at	1871 at	2634 at	4569 at	1873 at
	1089 cm^{-1}	1154 cm^{-1}	1403 cm^{-1}	1449 cm^{-1}	1589 cm^{-1}
633	16686 at	28115 at	20861 at	28651 at	16875 at
	1073 cm^{-1}	1142 cm^{-1}	1390 cm^{-1}	1436 cm^{-1}	1574 cm^{-1}
785	956 at	506 at	311 at	305 at	390 at
	1081 cm^{-1}	1146 cm^{-1}	1392 cm^{-1}	1434 cm^{-1}	1595 cm^{-1}

Table S10 Experimental frequencies (cm^{-1}) of fundamental vibrational bands of DMAB molecules within the wavelength range of 1000-1650 cm^{-1} .

Experimental frequencies / cm^{-1}	Assignments
1007	$\alpha\text{CCC}+\text{uCC}$
1081	$\text{uCC}+\text{uCS}$
1145	$\beta\text{C-H}+\text{uCN}$
1183	$\text{uCN}+\beta\text{C-H}+\text{uCC}$
1131	uCC
1391	$\text{uNN}+\text{uCC}+\beta\text{C-H}$
1428	$\text{uNN}+\text{uCC}+\beta\text{C-H}$
1489	$\beta\text{C-H}+\text{uNN}+\text{uCC}$
1591	uCC

u , α , and β denote the stretching coordinate, ring bending coordinate, and the in-plane bending coordinate out of the benzene ring, respectively.

Reference: Huang, Y. F.; Zhu, H. P.; Liu, G. K.; Wu, D. Y.; Ren B.; Tian, Z. Q. When the Signal Is Not from the Original Molecule To Be Detected: Chemical Transformation of para-Aminothiophenol on Ag during the SERS Measurement. *J. Am. Chem. Soc.* **2010**, *132*, 9244-9246.

Table S11 Summarized data of thicknesses of Ag shells of CS Au₁₂@Ag_t NPs with various Ag shell thickness, intensities of SERS band at 1080 cm⁻¹ of 4-ATP molecules on their films on glass substrates, comparisons of SPR intensity between Au and Ag, and the difference between t and $r/3$.

Diameters of Au cores (nm)	t (nm)	$r/3$ (nm)	Intensity of SERS band at 1080 cm ⁻¹	Comparisons of SPR intensity between Au and Ag	$t - (r/3)$ (nm)
12	1.1		1180	Au > Ag	-0.90
	1.8		2047	Au > Ag	-0.20
	2.1		5603	Au \approx Ag	0.10
	2.5	2.00	14104	Au < Ag	0.50
	2.9		14503	Au < Ag	0.90
	4.0		14584	Au < Ag	2.00
	4.6		14290	Au < Ag	2.60

Table S12 Summarized data of thicknesses of Ag shells of CS Au₂₀@Ag_t NPs with various Ag shell thickness, intensities of SERS band at 1080 cm⁻¹ of 4-ATP molecules on their films on glass substrates, comparisons of SPR intensity between Au and Ag, and the difference between t and $r/3$.

Diameters of Au cores (nm)	t (nm)	$r/3$ (nm)	Intensity of SERS band at 1080 cm ⁻¹	Comparisons of SPR intensity between Au and Ag	$t - (r/3)$ (nm)
20	1.5		2891	Au > Ag	-1.83
	2.1		4452	Au > Ag	-1.23
	2.8		9321	Au > Ag	-0.53
	3.7	3.33	16026	Au \approx Ag	0.37
	4.5		17021	Au < Ag	1.17
	5.5		18030	Au < Ag	2.17
	9.0		17818	Au < Ag	5.67

Table S13 Summarized data of thicknesses of Ag shells of CS Au₃₀@Ag_t NPs with various Ag shell thickness, intensities of SERS band at 1080 cm⁻¹ of 4-ATP molecules on their films on glass substrates, comparisons of SPR intensity between Au and Ag, and the difference between t and $r/3$.

Diameters of Au cores (nm)	t (nm)	$r/3$ (nm)	Intensity of SERS band at 1080 cm ⁻¹	Comparisons of SPR intensity between Au and Ag	$t - (r/3)$ (nm)
30	1.7	5.00	8112	Au>Ag	-3.30
	3.6		14275	Au>Ag	-1.40
	5.0		19435	Au>Ag	0.00
	6.4		20803	Au<Ag	1.40
	9.8		22577	Au<Ag	4.80
	12.0		26990	Au<Ag	7.00

Table S14 Summarized data of thicknesses of Ag shells of CS Au₄₅@Ag_t NPs with various Ag shell thickness, intensities of SERS band at 1080 cm⁻¹ of 4-ATP molecules on their films on glass substrates, comparisons of SPR intensity between Au and Ag, and the difference between t and $r/3$.

Diameters of Au cores (nm)	t (nm)	$r/3$ (nm)	Intensity of SERS band at 1080 cm ⁻¹	Comparisons of SPR intensity between Au and Ag	$t - (r/3)$ (nm)
45	0		5826	Au>Ag	-7.50
	0.9		9761	Au>Ag	-6.60
	1.5		13850	Au>Ag	-6.00
	2.9	7.5	16806	Au>Ag	-4.60
	5.5		17763	Au>Ag	-2.00
	8.2		18559	Au>Ag	0.70
	11.0		21016	Au>Ag	3.5

Table S15 Summarized data of thicknesses of Ag shells of CS Au₅₅@Ag_t NPs with various Ag shell thickness, intensities of SERS band at 1080 cm⁻¹ of 4-ATP molecules on their films on glass substrates, comparisons of SPR intensity between Au and Ag, and the difference between t and $r/3$.

Diameters of Au cores (nm)	t (nm)	$r/3$ (nm)	Intensity of SERS band at 1080 cm ⁻¹	Comparisons of SPR intensity between Au and Ag	$t - (r/3)$ (nm)
55	0	9.17	6533	Au>Ag	-9.17
	0.8		8739	Au>Ag	-8.37
	2.7		18983	Au>Ag	-6.47
	5.0		18977	Au>Ag	-0.55
	10.0		19840	Au>Ag	0.83
	16.0		22334	Au>Ag	6.83